Biosensors and Bioelectronics 135 (2019) 129–136

Contents lists available at ScienceDirect

Biosensors and Bioelectronics

journal homepage: www.elsevier.com/locate/bios

Direct quantification of cancerous exosomes via surface plasmon resonance with dual gold nanoparticle-assisted signal amplification

Qing Wang[a], Liyuan Zou[a], Xiaohai Yang[a,*], Xiaofeng Liu[a], Wenyan Nie[a], Yan Zheng[a], Quan Cheng[b], Kemin Wang[a,**]

[a] State Key Laboratory of Chemo/Biosensing and Chemometrics, College of Chemistry and Chemical Engineering, Key Laboratory for Bio-Nanotechnology and Molecular Engineering of Hunan Province, Hunan University, Changsha, 410082, China
[b] Department of Chemistry, University of California, Riverside, CA, 92521, United States

ARTICLE INFO

Keywords:
Exosomes
Surface plasmon resonance
Aptasensor
AuNP

ABSTRACT

Sensitive detection of cancerous exosomes is critical to early diseases diagnosis and prognosis. Herein, a sensitive aptasensor was demonstrated for exosomes detection by surface plasmon resonance (SPR) with dual gold nanoparticle (AuNP)-assisted signal amplification. Dual nanoparticle amplification was achieved by controlled hybridization attachment of AuNPs resulting from electronic coupling between the Au film and AuNPs, as well as coupling effects in plasmonic nanostructures. By blocking the Au film surface with 11-Mercapto-1 -undecanol (MCU), nonspecific adsorption of AuNPs onto the SPR chip surface was suppressed and regeneration of the SPR sensor was realized. This method was highly sensitive and we have achieved the limit of detection (LOD) down to 5×10^3 exosomes/mL, which showed a 10^4-fold improvement in LOD compared to commercial ELISA. Moreover, the SPR sensor had the capability to differentiate the exosomes secreted by MCF-7 breast cancer cells and MCF-10A normal breast cells. Furthermore, the SPR sensor could effectively detect the exosomes in 30% fetal bovine serum. The work provides a sensitive and efficient quantification approach to detect cancerous exosomes and offers an avenue toward future diagnosis and comprehensive studies of exosomes.

1. Introduction

Exosomes are nano-sized extracellular vesicles with sizes ranging from 30 nm to 150 nm that are released from the cell by fusion of multivesicular bodies with the plasma membrane (Théry et al., 2002; Raposo and Stoorvogel, 2013). Due to their cellular origin, exosomes carry a number of molecules of interest including transmembrane proteins CD63 (Li et al., 2017a; Jakobsen et al., 2015), lipids (Subra et al., 2007) and a series of nucleic acids (Fang et al., 2018; Lee et al., 2015). Owing to their crucial role as conveyors in cell-cell communication (Théry et al., 2009; Mathivanan et al., 2010), cancer metastasis (Steinbichler et al., 2017) and liquid biopsy (Chi, 2016), these tumor-derived exosomes, provide a promising biomarker resource for early tumor diagnosis and monitoring of diseases without the need to invasively access the tumor.

Although there were a number of techniques available for qualitative analysis on exosomes, biomarker study using exosomes remains challenging. Electron microscopy (Wubbolts et al., 2003; Théry et al., 2006) may provide information on size and morphology of exosomes, but this approach cannot effectively provide quantitative information because of exosomes loss during dehydration and embedding process. Immunoaffinity-based approaches (Hosseini-Beheshti et al., 2012; Jakobsen et al., 2015), such as enzyme-linked immunosorbent assays (ELISA), could identify typical markers of exosomal proteins for exosomes detection. However, these methods required expensive labelling and showed poor sensitivity. To date, methods taking advantage of direct particle counting have become popular. For example, nanoparticle tracking analysis (NTA) (Filipe et al., 2010) became an ideal tool to count and sort exosomes via light scattering in a liquid suspension. Unfortunately, this method has a limited working range for exosomes concentration measurements (only 10^6 to 10^9 exosomes per mL), and it fails to identify well-defined exosomes subpopulations characterized in the presence of specific exosomal markers. Other novel approaches such as microfludics (Wunsch et al., 2016; Ibsen et al., 2017), electroanalytical assay (Doldán et al., 2016; Li et al., 2017b), surface-enhanced Raman scattering (SERS) (Park et al., 2017), cantilever array sensor (Etayash et al., 2016), surface plasmon resonance (SPR) (Di Noto et al., 2016; Thakur et al., 2017; Zhu et al., 2014) and

* Corresponding author.
** Corresponding author.
E-mail addresses: yangxiaohai@hnu.edu.cn (X. Yang), kmwang@hnu.edu.cn (K. Wang).

https://doi.org/10.1016/j.bios.2019.04.013
Received 19 October 2018; Received in revised form 16 March 2019; Accepted 5 April 2019
Available online 13 April 2019
0956-5663/

mass spectrometry (Zou et al., 2017) have been reported. Generally, most of these methods utilized antibodies specific to the exosomal surface proteins. Although specific, antibodies are expensive, cannot be produced by a chemical process, require demanding storage conditions, and might interfere with immunogenicity when used in therapeutic applications.

Aptamers are specific oligonucleotide molecules (Tuerk and Gold, 1990). As a promising and effective alternative to antibodies for targeted recognition, these "chemical antibodies" exhibit excellent specificity and binding affinity toward specific targets (Jiang et al., 2017). Moreover, aptamers are less likely to provoke undesirable immune responses. Zhou et al. reported an electrochemical strategy to detect exosomes with aptamers. In the presence of exosomes, exosomes displaced the probing strand with methylene blue and caused an electrochemical signal to change (Zhou et al., 2016a). Moreover, colorimetric aptasensors (Xia et al., 2017; Wang et al., 2017c) taking advantage of specific aptamer of CD63 offered visible and low-cost methods for exosomes analysis. Zhou et al. introduced a multiplexed electrochemical sensor for circulating exosomes detection based on metal nanoparticles (Zhou et al., 2016b). Wang et al. developed a SERS method for multiple detection of cancer exosomes (Wang et al., 2018). Given that the concentration of exosomes in the early stage of the disease was extremely low, highly sensitive method for exosomes detection was required. Wang et al. reported a sensitive electrochemical method to quantify tumor-derived exosomes using artificial nucleotide (Wang et al., 2017b). But this artificial nucleobase-containing aptamer is expensive and difficult to synthetize. Thus, it was necessary to develop sensitive aptasensors for exosomes analyses.

Herein, an aptamer-based SPR sensor for direct and sensitive detection of exosomes was reported. Fig. 1 showed the results of detecting target exosomes by direct measurement, single gold nanoparticle (AuNP) amplified SPR aptasensor, and dual AuNP amplified SPR aptasensor, respectively. Firstly, the Au film was functionalized with capture DNA and the target exosomes were detected by direct measurement. Then aptamer/T_{30} linked AuNPs were added and target exosomes were detected by single AuNP amplified SPR aptasensor. Finally, A_{30} coated AuNPs could be captured on the aptamer/T_{30} linked AuNPs through the hybridization of two complementary sequences (T_{30} and A_{30}), and target exosomes were detected by dual AuNP amplified SPR aptasensor. Utilizing dual AuNP-assisted signal amplification, detection of exosomes in the low concentration was achieved. This method provided an effective way for sensitive exosomes detection, and is a promising technical for applications in biological and clinical studies.

2. Experimental

2.1. Chemical reagents

All oligonucleotides were purchased from Shanghai Sangon Biotechnology Co. (China), including capture DNA (5′-CACCCCACCTC GCTCCCGTGACACTAATGCTATTTTT-HS-3′), CD63 aptamer (5′-CACC CCACCTCGCTCCCGTGACACTAATGCTA-HS-3′), T_{30} (5′-SH-T_{30}-3′) and A_{30} (5′-SH-A_{30}-3′). 11-Mercapto-1-undecanol (MCU), 6-Mercapto-1-hexanol (MCH) and sodium dodecyl sulfate (SDS) were purchased from Sigma-Aldrich (USA). All of the solutions were prepared using ultrapure

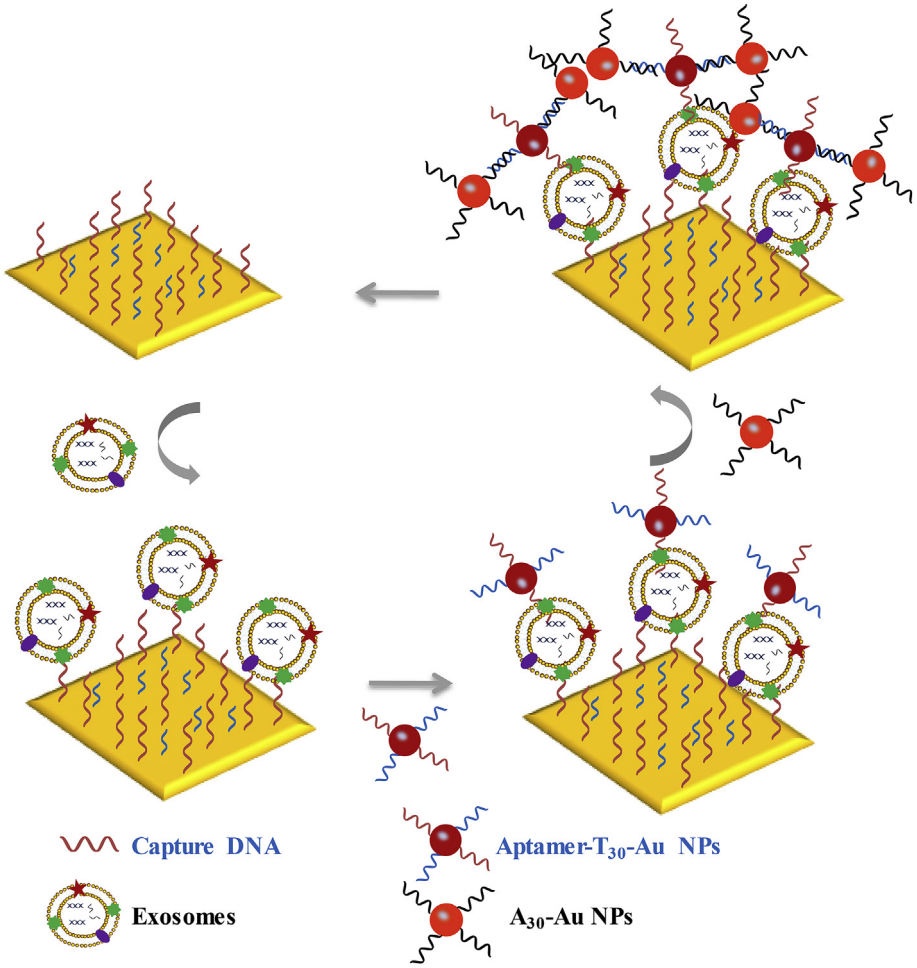

Fig. 1. Dual AuNP-assisted signal amplification for determination of exosomes.

water.

2.2. Preparation and modification of AuNPs

AuNPs (~13 nm) were prepared according to procedures described previously by citrate reduction of $HAuCl_4$ (Nie et al., 2017; Wang et al., 2017a). DNA-linked AuNPs, including aptamer/T_{30} linked AuNPs conjugates and A_{30} coated AuNPs conjugates, were prepared following the method described in our previous work (Liu et al., 2017; Wang et al., 2016a). Briefly, for aptamer/T_{30} linked AuNPs, 9 μL of 100 μM thiol-modified aptamer and T_{30} were added to 882 μL of AuNPs solution. The solution was then kept at 4 °C for 16 h followed by addition of 50 mM PBS (pH 7.0, 0.5 M NaCl). After aging at 4 °C for 48 h, the solution was centrifuged at 13,000 rpm for 30 min with the removal of excess reagents and resuspension of the pellet in 10 mM PBS (pH 7.0, 137 mM NaCl). This step was repeated three times. After the final centrifugation, the pellet was dispersed in 10 mM PBS. UV−vis spectroscopy (Shimadzu, Japan) was used for further characterization. The absorption spectrum of unmodified AuNPs and DNA-AuNPs showed peak at about 518.0 nm and 524.0 nm (Fig. S-1). The median hydrodynamic diameter of unmodified AuNPs and DNA-linked AuNPs by dynamic light scattering (DLS) were 21.9 nm and 39.4 nm. The results of UV and DLS showed that DNA-AuNPs were prepared successfully (Fig. S-2).

2.3. Cell culture

All cells were incubated in a humidified atmosphere containing 5% CO_2 at 37 °C. Breast cancer cells MCF-7 were cultured in high-glucose Dulbecco's modified eagle medium (DMEM) with 10% exosome-depleted FBS. Normal breast cell lines MCF-10A were cultured in mammary epithelial cell growth medium (MEGM) containing 5% exosomes-depleted horse serum and cholera toxin.

2.4. Exosomes isolation and characterization

Exosomes derived from MCF-7 cells or MCF-10A cells were collected from the cell culture supernatant after 48 h culture based on a multi-step centrifugation protocol with some modification (Zhou et al., 2016b). In brief, the cell debris and the large microvesicles were eliminated by centrifugation for 10 min at 2000 g and by the second centrifugation at 10,000 g for 60 min. The exosomes-containing supernatant was filtered using a 0.22-μm filter. Subsequently, the filtered media were ultracentrifuged at 100,000 g for 2.5 h at 4 °C to precipitate the exosomes. The resulting sediment was collected as exosomes. The sediment was washed with PBS, and centrifuged again at 100,000 g for 2.5 h at 4 °C. Finally, the collected exosomes were resuspended in 10 mM PBS for further use.

The morphology of the purified MCF-7 exosomes was obtained using a Tecnai20 transmission electron microscope (FEI., USA). The size distribution of the exosomes was performed using a Zetasizer Nano ZS90 (Malvern Instruments, U.K.). The concentrations of the exosomes were obtained by NS 300 instrument (Malvern Instruments, U.K.). Exosomal markers (CD9 and CD63) were identified using Western blot analysis.

2.5. Surface modification of Au film

Surface modification of the sensor chip was achieved according to previous work (Wu et al., 2016; Wang et al., 2016b; Yi et al., 2013). In brief, Au film was firstly cleaned. Then, the chip was soaked in freshly prepared 7:3 H_2SO_4/H_2O_2 (piranha solution) for 1 min, followed by rinsing with ultrapure water. Then, 5 μM capture DNA was applied to the chip at 4 °C. After surface modification of the sensor chip, the film was blocked with 2 mM MCH or MCU for 3 h. Unbound MCH or MCU was thoroughly washed away with 10 mM PBS.

2.6. Surface plasmon resonance measurements

The SPR experiments were performed with a time-resolved EC-SPR device (Dingcheng Technology, Changchun, China). Exosomes were then injected into the Au film surface and incubated with the capture aptamers for 1 h. After binding, the surface was rinsed thoroughly with PBS. Then, aptamer/T_{30} linked AuNPs were injected and incubated for 50 min. Next, A_{30} coated AuNPs were incubated for 45 min. After washing repeatedly with PBS, the SPR resonance angle was recorded. Based on the change of resonance angle after binding and washing, the concentration of exosomes could be determined. Finally, the surface was regenerated with regeneration solution (0.1% SDS/10 mM NaOH) for subsequent detection.

2.7. Exosomes detection in complex samples

The preparation of the serum sample was achieved according to the previous work (Doldán et al., 2016). Fetal bovine serum (FBS) was first ultracentrifuged at 100,000 g for 2.5 h at 4 °C to remove the exosomes of FBS. The purified exosomes from MCF-7 cells were then added in 20% or 30% FBS. Next, the above exosomes samples were detected. The detection procedure in FBS samples was the same as that in the buffer.

3. Results and discussion

3.1. Characterization of exosomes and selection of the passivation reagent

Exosomes were first characterized by transmission electron micrograph (TEM), DLS and NTA. The morphology of the purified exosomes was obtained by TEM and the result illustrated that the purified exosomes demonstrated an average size of ca. 90 nm with good structure integrity. (Fig. 2A and B). The median hydrodynamic diameter of exosomes by DLS (Fig. 2C) was ca. 92 nm, which was consistent with TEM result. And the concentration of exosomes measured by NTA was 2.5×10^{10} exosomes/mL (Fig. 2D). In addition, the expression of CD9 and CD63 was analyzed via Western blotting analysis. Specific bands of CD9 and CD63 were presented in Fig. 2E. These findings corroborated the previous work for characterization of exosomes (Jiang et al., 2017; Wang et al., 2017c).

This method involved dual AuNP-assisted signal amplification. In order to avoid the nonspecific adsorption of nanoparticles onto SPR chip surface, different blocking reagents (MCH or MCU) were immobilized onto Au film surface, respectively. As showed in Fig. 3A, for MCH blocked Au film, $\triangle\theta$ was less than 0.0015° when aptamer/T_{30} linked AuNPs were added, indicating that MCH could prevent the nonspecific adsorption of aptamer/T_{30} linked AuNPs on the Au film surface effectively. However, $\triangle\theta$ was 0.1000° when A_{30} coated AuNPs were added, suggesting that MCH was not effective to prevent the nonspecific adsorption of A_{30} coated AuNPs. For MCU blocked Au film, no matter what aptamer/T_{30} linked AuNPs or A_{30} coated AuNPs were added, the resonance angle had nearly no shift suggesting that MCU was a better passivation agent.

This method involved dual AuNP-assisted signal amplification, so it was necessary to avoid the background signal resulted from these two kinds of AuNPs, i.e A_{30} coated AuNPs and aptamer/T_{30} linked AuNPs. On the one hand, the background signal was resulted from the non-specific adsorption of these two kinds of AuNPs on the Au film. On the other hand, the background signal may be caused by the hybridization of the capture DNA modified on the chip surface with oligonucleotide modified on the AuNPs. If the capture DNA did not use T_5 as the linker, obvious resonance angle change was observed when aptamer/T_{30} linked AuNPs or A_{30} coated AuNPs was added in the absent of block reagent, suggesting that these two kinds of AuNPs could be non-specifically adsorbed on the Au film. Both MCH and MCU have similar performance in decreasing the background signal resulted from these two kinds of AuNPs (Fig. 3A). However, given that capture DNA

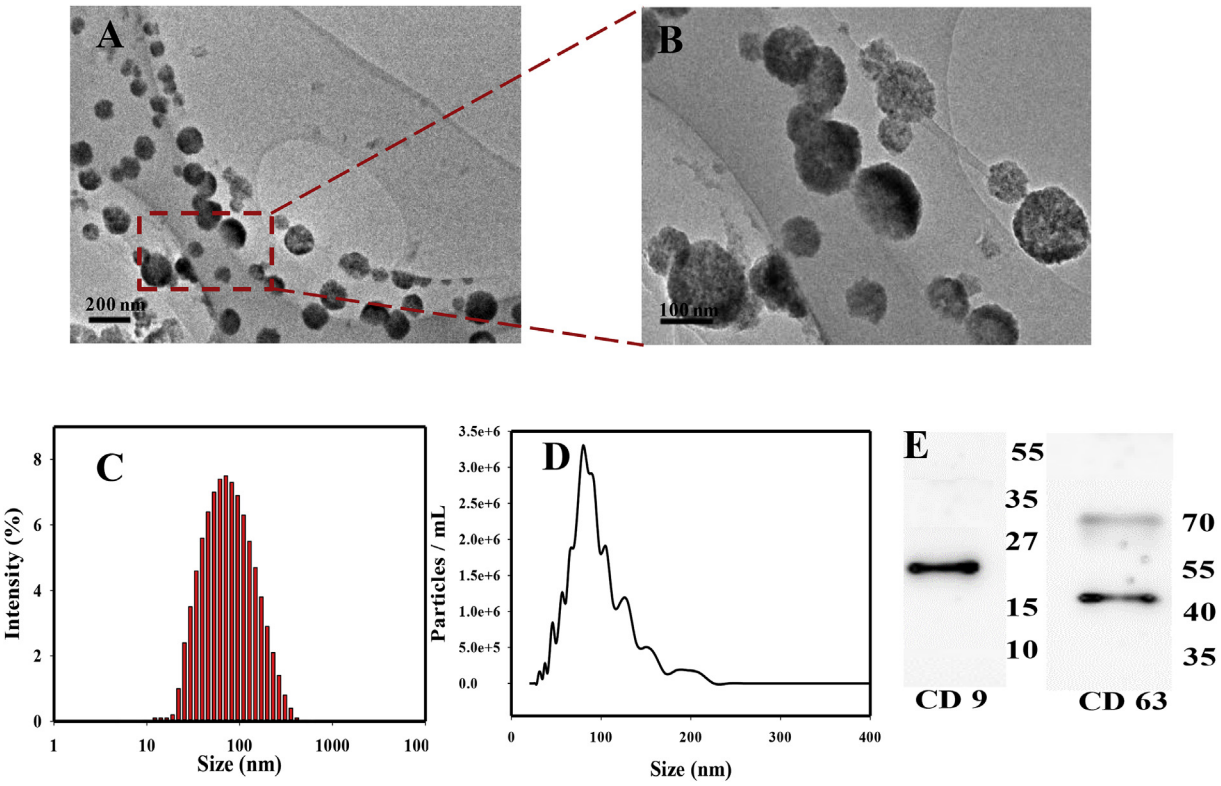

Fig. 2. TEM images (A and B), DLS size distribution (C), NTA (D) and Western blot (E) of exosomes.

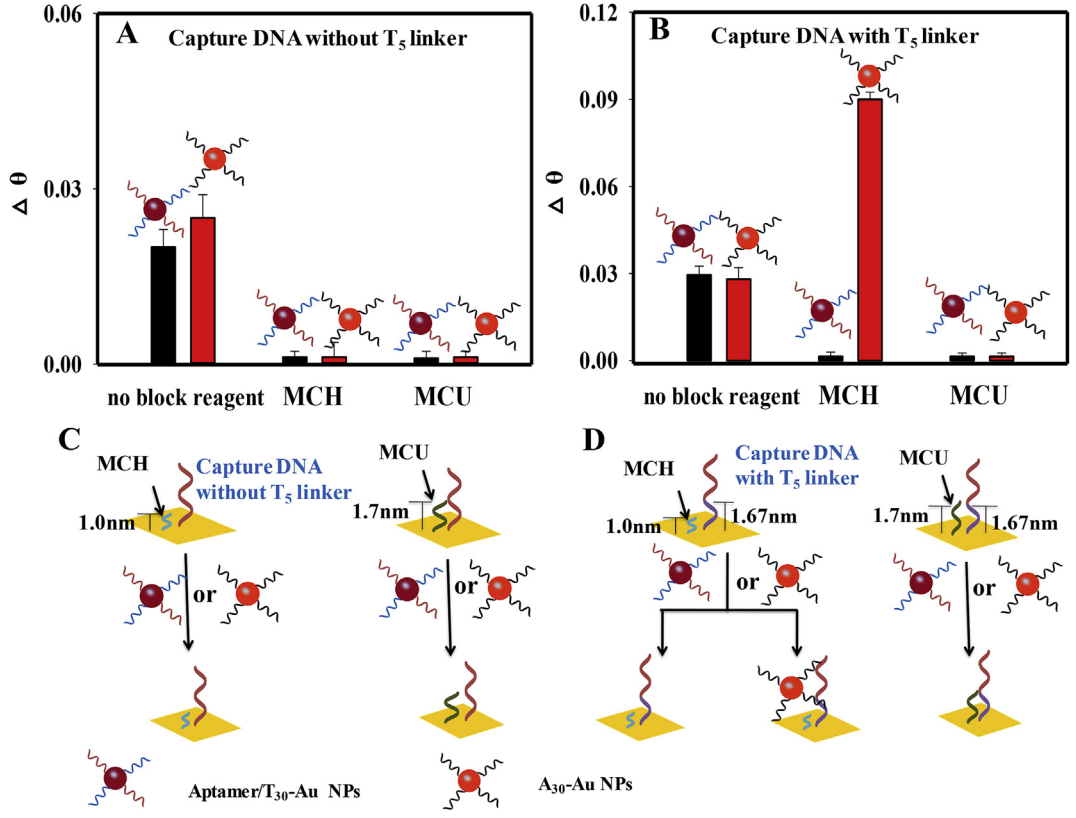

Fig. 3. SPR response of (A) capture DNA (without T_5 as linker) modified Au film and (B) capture DNA (with T_5 as linker) modified Au film when aptamer/T_{30} linked AuNPs or A_{30} coated AuNPs were added in the absence or present of block reagent (MCH or MCU); Schematic illustration of (C) capture DNA (without T_5 as linker) modified Au film and (D) capture DNA (with T_5 as linker) modified Au film when aptamer/T_{30} linked AuNPs or A_{30} coated AuNPs were added in the present of MCH or MCU.

without T_5 showed a weaker SPR response than with T_5 in the present of target exosomes (Fig. S-3), capture DNA with T_5 was utilized in our work. As showed in Fig. 3B, if the capture DNA use T_5 as the linker, these two kinds of AuNPs could also be nonspecifically adsorbed on the Au film in the absent of block reagent. For MCH blocked Au film, △θ was less than 0.0015° when aptamer/T_{30} linked AuNPs were added, indicating that MCH could prevent the nonspecific adsorption of aptamer/T_{30} linked AuNPs on the Au film surface effectively. However, △θ was 0.1000° when A_{30} coated AuNPs were added, suggesting that MCH was not effective to prevent the nonspecific adsorption of A_{30} coated AuNPs. For MCU blocked Au film, no matter what aptamer/T_{30} linked AuNPs or A_{30} coated AuNPs were added, the resonance angle had nearly no shift suggesting that MCU was a better passivation agent.

Both MCH and MCU could make DNA molecules stand on the surface and block the Au film (Wang et al., 2016b). The theoretical lengths of these passivation agents were 1.0 nm (MCH) (Yang et al., 2017) and 1.7 nm (MCU) (Asakawa et al., 2017), respectively (Fig. 3C and D). Thiol-modified capture DNA was a sequence of CD63 aptamer with T_5. Moreover, the theoretical length of T_5 was about 1.67 nm (Wang et al., 2016c), which was equivalent to the length of MCU but much longer than MCH. Presumably, the length of MCU was equivalent to the length of T_5, so the MCU layer could hinder the hybridization of capture DNA with A_{30} coated AuNPs. While the length of MCH was shorter than that of T_5, so the MCH could not effectively prevent the hybridization of capture DNA with A_{30} coated AuNPs. MCU suppresses nonspecific adsorption of nanoparticles effectively and was thus selected for the detection experiments.

3.2. Feasibility study and optimization of experimental conditions

The feasibility of the dual AuNP-assisted SPR sensor was studied. As shown in Fig. 4A, as 10^9 exosomes/mL target exosomes were reacted with capture CD63 aptamer modified Au film, △θ (0.0260°) was obtained (curve 1 to 2). Then aptamer/T_{30} linked AuNPs were added, △θ (0.1075°) was observed (curve 2 to 3) indicating that the aptamer/T_{30} linked AuNPs were captured on the free region of the captured exosomes. After the A_{30} coated AuNPs were injected, △θ (0.1910°) was obvious (curve 3 to 4), suggesting that the A_{30} coated AuNPs were hybridized with aptamer/T_{30} linked AuNPs. And the in situ SPR sensorgram was showed in Fig. 4B. This result demonstrated that the dual AuNP-assisted SPR aptasensor was beneficial to signal enhancement. In addition, when the sensor chip was incubated with regeneration solution, the SPR curve moved from curve 4 to 5. Moreover, the resonance angle after regeneration was generally coincident with curve 1, indicating that regeneration of the Au film was fulfilled through regeneration solution.

The surface was also characterized using atomic force microscopy (SP13800N SPA400, Seiko, Japan). As shown in Fig. S-4 of Supporting Information, if only the aptamer/T_{30} linked AuNPs and A_{30} coated AuNPs were injected, no obvious change could be observed for AFM image of the Au surface (from Fig. S–4A to Fig. S–4B). However, when target exosomes, the aptamer/T_{30} linked AuNPs and A_{30} coated AuNPs were step by step added, it showed that target exosomes were captured on the chip, and then AuNPs were captured on the exosomes surface (shown in Fig. S–4C).

The experimental conditions, such as the surface density of the capture DNA, the incubation time of exosomes, the incubation time of aptamer/T_{30} linked AuNPs with exosomes, and the incubation time of A_{30} coated AuNPs with aptamer/T_{30} linked AuNPs were investigated to achieve the optimal performance for detecting cancerous exosomes. First, by incubating 1 μM, 5 μM and 10 μM of the capture DNA with the sensor chip, 1.88×10^{12} molecules/cm^2, 5.65×10^{12} molecules/cm^2 and 1.02×10^{13} molecules/cm^2 surface was acquired. The surface density of DNA was calculated by chronocoulometry (Wang et al., 2016b). As shown in Fig. S–5A, the largest SPR response could be acquired at 5.65×10^{12} molecules/cm^2. Thus 5 μM of the capture DNA was chosen for the following experiments. As shown in Fig. S–5B, SPR response increased along with the increase of the incubation time of exosomes, and was stable in 60 min. Therefore, the optimal time for exosomes incubation was set at 60 min. The incubation time of aptamer/T_{30} linked AuNPs and A_{30} coated AuNPs were also investigated. The optimal time for aptamer/T_{30} linked AuNPs and A_{30} coated AuNPs were 50 min and 45 min, respectively (Figs. S–5C and S–5D).

3.3. Exosomes detection using the dual AuNP-assisted SPR aptasensor

To further demonstrate quantitation of cancer biomarkers by the dual AuNP-assisted SPR strategy, SPR analysis of MCF-7 cells-derived exosomes were carried out with a series of concentrations. As showed in Fig. S-6, the resonance shift caused by blank sample was 0.0010°. Given that a shift of resonance angle larger than 0.0015° was considered as signal for the SPR instrument, no SPR signal was observed for blank sample. Fig. 5A indicated that the SPR signal gradually increased when the exosomes concentration increased through dual AuNP amplified SPR strategy. Fig. 5B presented the comparison of SPR signals obtained by direct exosomes measurement, single AuNP amplified SPR aptasensor, and dual AuNP amplified SPR aptasensor. As shown in Fig. S-7, the correlation equation was $\Delta\theta = 0.01641\lg C - 0.1082$ ($R^2 = 0.99$), $\Delta\theta = 0.01665\lg C - 0.08165$ ($R^2 = 0.96$) and $\Delta\theta = 0.0231\lg C - 0.0874$ ($R^2 = 0.99$), respectively. According to 3σ rules, the limit of detection (LOD) of direct exosomes measurement, single AuNP amplified SPR aptasensor, and dual AuNP amplified SPR aptasensor was estimated 6.5×10^7 exosomes/mL, 1.0×10^5 exosomes/mL and 5.0×10^3exosomes/mL, respectively. The LOD for the dual AuNP-

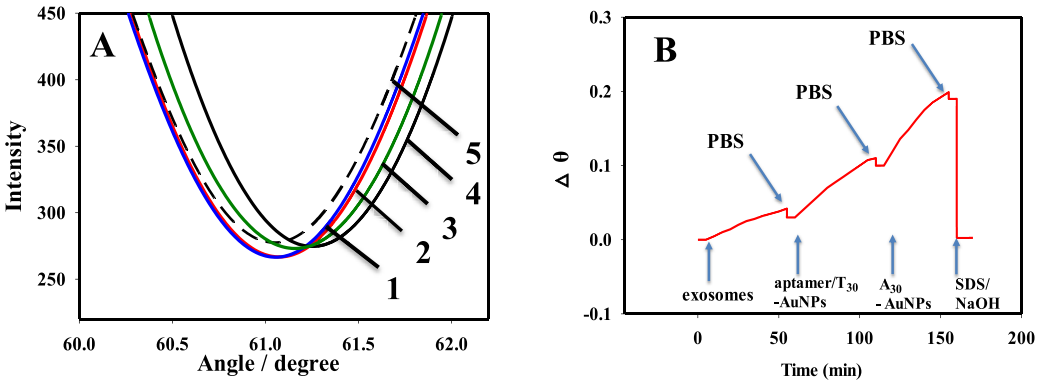

Fig. 4. (A)SPR spectra of (1) aptamer modified Au film; (2) 10^9 exosomes/mL target exosomes; (3) reaction with the aptamer/T_{30} linked AuNPs; (4) reaction with the A_{30} coated AuNPs; (5) regeneration. (B) SPR response in situ of the dual AuNP-assisted SPR sensor.

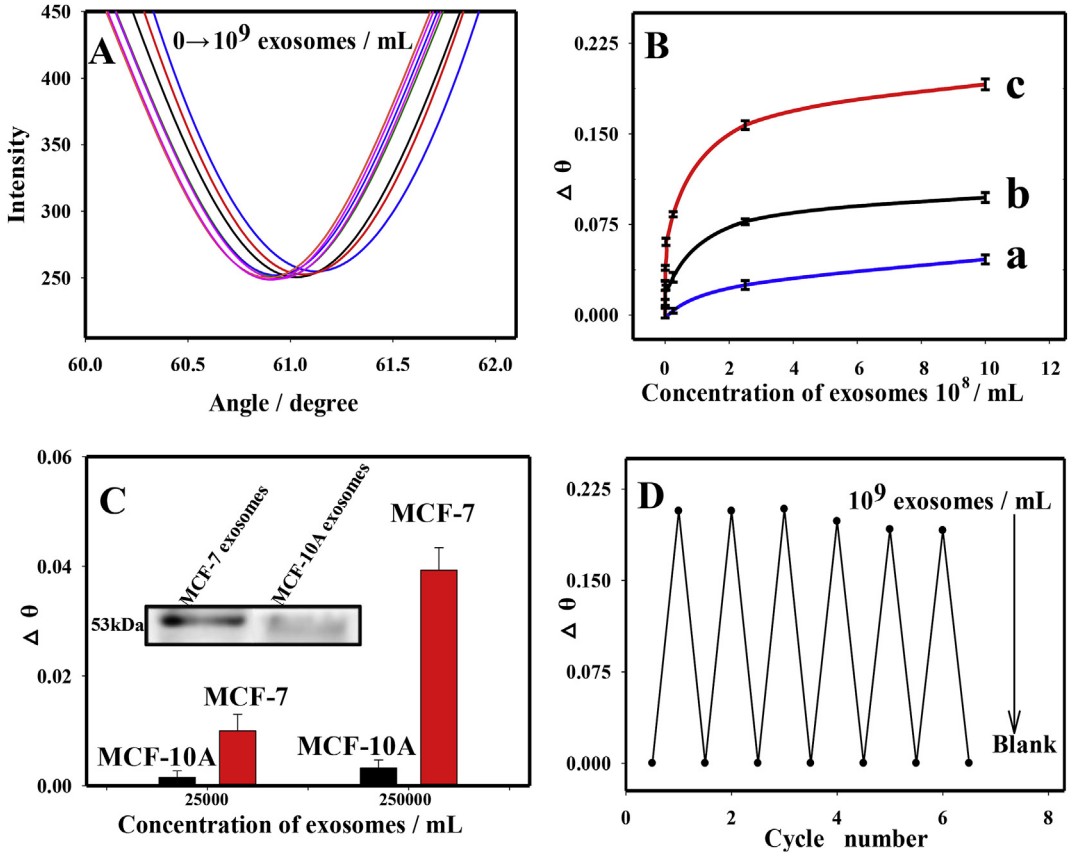

Fig. 5. (A) SPR spectra of different concentrations of exosomes. (B) The relationship between Δθ and exosomes concentrations by using different sensing strategies. Error bars showed the standard deviation of the measurements that were performed in triplicate. (a) direct measurement, (b) single AuNP amplified SPR aptasensor, (c) dual AuNP amplified SPR aptasensor. (C) Selectivity assessment comparing cancerous MCF-7 cells-derived exosomes and non-cancerous MCF-10a cells-derived exosomes. Inserted figure: Western blot analysis of 10^9/mL MCF-7 cells-derived exosomes and MCF-10 cells-derived exosomes. (D) Reproducibility investigation of the SPR biosensor. The sensor chip was regenerated by 0.1% SDS/10 mM NaOH solution for 5 min.

Table 1
Comparison of LODs of different methods for exosomes detection.

No.	Method	LOD (exosomes/mL)	Reference
1	Aptamer-based electrochemical biosensor	1×10^6	Zhou et al. (2016a)
2	Aptasensor based on DNA-capped s-SWCNTs	5.2×10^8	Xia et al., 2017
3	Electrochemical sensor with metal nanoparticles	5×10^4	Zhou et al. (2016b)
4	Aptasensor based on g-C_3N_4 nanosheets	1.35×10^9	Wang et al. (2017c)
5	Electrochemical sensor with expanded nucleotide	2.09×10^4	Wang et al. (2017b)
6	Electrochemical sandwich immunosensor	2.0×10^5	Doldán et al., 2016
7	Nanomechanical sandwich assay	200	Etayash et al. (2016)
8	Concentration-Normalized electroanalysis	1.9×10^5	Li et al. (2017b)
9	dual AuNP amplified SPR aptasensor	5×10^3	This work

assisted SPR aptasensor was 20 times lower than that of SPR amplified by single AuNP. Signal enhancement may be caused by the following reasons. Firstly, as the exosome was present, DNA modified AuNPs could be assembled on the Au film, resulting in the increase of dielectric constant of the dielectric layer (Wang et al., 2016b). Secondly, aptamer/T_{30} linked AuNPs could capture many A_{30} coated AuNPs by DNA hybridization, and it resulted in coupling effects in plasmonic nanostructures (Baek et al., 2014; Liu and Liedl, 2018). Thirdly, electronic coupling between surface plasmon wave with Au film and the localized plasmon of AuNPs led to enhancement of SPR signal (He et al., 2004). In Table 1, currently available approaches for exosomes detection were listed. Clearly, the LOD of the dual AuNP-assisted aptasensor was lower than most of the current aptamer-based methods.

The capability of the sensor chip to differentiate the exosomes secreted by MCF-7 cells and MCF-10A cells was then assessed. The exosomes were firstly characterized using Western blot analysis. As shown in the inserted figure of Fig. 5C, it showed that the exosome marker CD63 was present in MCF-7 cells-derived exosomes and MCF-10 cells-derived exosomes, which was consistent with the previous paper (Zhang et al., 2017). In addition, the protein expression of CD63 was higher in MCF-7 cells-derived exosomes. As shown in Fig. 5C, there was a clear Δθ change in the case of exosomes produced from the MCF-7 cells, while Δθ was much weaker in MCF-10A cells-derived exosomes. Take 2.5×10^5 exosomes/mL as an example, Δθ was 0.0393° for MCF-7 cells-derived exosomes, which was 10 times larger than MCF-10A cells-derived exosomes (0.0032°). The result of SPR sensor was also similar to that of Western blot. Moreover, the result was also consistent with the previously reported work (Xia et al., 2017; Wang et al., 2017c), which proved that this dual AuNP-assisted SPR aptasensor showed satisfactory selectivity to cancerous exosomes and normal cells-derived exosomes.

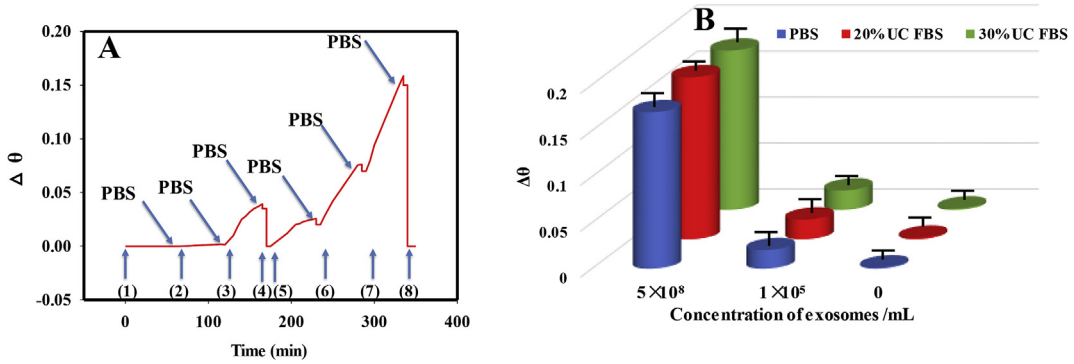

Fig. 6. (A) SPR response in 30% UC FBS. (1) adding 1×10^5 exosomes/mL; (2) adding aptamer/T_{30} linked AuNPs; (3) adding A_{30} coated AuNPs; (4) adding 0.1% SDS/10 mM NaOH; (5) adding 5×10^8 exosomes/mL; (6) adding aptamer/T_{30} linked AuNPs; (7) adding A_{30} coated AuNPs; (8) adding 0.1% SDS/10 mM NaOH. (B) Detection of exosomes in 10 mM PBS (blue histogram), 20% UC FBS (red histogram) and 30% UC FBS (green histogram). (For interpretation of the references to color in this figure legend, the reader is referred to the Web version of this article.)

The reproducibility of the SPR sensor was also of great importance. We further tested the reproducibility of the dual AuNP-assisted SPR aptasensor (Fig. 5D). After a round of analysis of sample, the chip was regenerated for subsequent detection. When the dual AuNP-assisted aptasensor was used to detect 10^9 exosomes/mL MCF-7 cells-derived exosomes, there was no significant signal weakening for six cycles and the relative standard deviation was 3.3%, which suggested the dual AuNP-assisted SPR aptasensor showed good reproducibility.

3.4. Detection of exosomes in complex samples

To assess the real application of dual AuNP-assisted SPR aptasensor for detecting cancerous exosomes, the MCF-7 cells-derived exosomes were quantified in fetal bovine serum (FBS). Given that serum contains an abundance of compositions apart from exosomes, ultra-centrifuged (UC) FBS as an artificial system was introduced to evaluate the performance of this SPR aptasensor. As shown in Fig. 6A, the curve remained stable when injecting 1×10^5 exosomes/mL MCF-7 cells-derived exosomes, indicating that the concentration of exosomes was too low to detect. The SPR response increased greatly when the aptamer/T_{30} linked AuNPs and A_{30} coated AuNPs was added. Next the chip was regenerated with regeneration solution for subsequent detection. When 5×10^8 exosomes/mL MCF-7 cells-derived exosomes was added, small SPR response could be obtained. Similarly, obvious enhancement of SPR response could be achieved as the aptamer/T_{30} linked AuNPs and A_{30} coated AuNPs was added. The chip could also be regenerated using regeneration solution. As shown in Fig. 6B, whether in 10 mM PBS or in 20% and 30% UC FBS, the SPR signal caused by the target exosomes was almost the same. Consequently, it suggested that the SPR aptasensor had a good performance in complex sample and possessed potential for future application.

4. Conclusions

In summary, a SPR aptasensor based on dual AuNP-assisted signal amplification was developed for direct and highly sensitive detection of exosomes. Due to the electronic coupling and the coupling effects in plasmonic nanostructures, the LOD of the dual AuNP-assisted SPR aptasensor was lowered to 5×10^3 exosomes/mL. Moreover, the dual AuNP-assisted SPR aptasensor showed satisfactory regeneration, acceptable selectivity and good reproducibility. This enzyme-free method offered opportunities for the development of exosomes quantification. The work might provide a sensitive and effective method for exosomes-based disease diagnostics and clinical analyses.

Declaration of interests

The authors declare that they have no known competing financial interests or personal relationships that could have appeared to influence the work reported in this paper.

CRediT authorship contribution statement

Qing Wang: Funding acquisition, Project administration, Writing - review & editing. **Liyuan Zou:** Writing - original draft, Data curation, Validation, Visualization. **Xiaohai Yang:** Conceptualization, Supervision, Methodology. **Xiaofeng Liu:** Resources, Investigation. **Wenyan Nie:** Validation, Visualization. **Yan Zheng:** Validation, Investigation. **Quan Cheng:** Writing - review & editing. **Kemin Wang:** Funding acquisition, Project administration.

Acknowledgments

This work was supported by the National Natural Science Foundation of China (21675047, 21375034 and 21735002), and National Science Foundation for Distinguished Young Scholars of Hunan Province (2016JJ1008).

Appendix A. Supplementary data

Supplementary data to this article can be found online at https://doi.org/10.1016/j.bios.2019.04.013.

References

Asakawa, H., Inada, N., Hirata, K., Matsui, S., Igarashi, T., Oku, N., Yoshikawa, N., Fukuma, T., 2017. Nanotechnology 28, 455603.
Baek, S.H., Wark, A.W., Lee, H.J., 2014. Anal. Chem. 86, 9824–9829.
Chi, K.R., 2016. Nature 532, 269–271.
Di Noto, G., Bugatti, A., Zendrini, A., Mazzoldi, E.L., Montanelli, A., Caimi, L., Marco, R., Doris, R., Bergese, P., 2016. Biosens. Bioelectron. 77, 518–524.
Doldán, X., Fagúndez, P., Cayota, A., Laíz, J., Tosar, J.P., 2016. Anal. Chem. 88, 10466–10473.
Etayash, H., McGee, A.R., Kaur, K., Thundat, T., 2016. Nanoscale 8, 15137–15141.
Fang, T., Lv, H., Lv, G., Li, T., Wang, C., Han, Q., Cao, D., 2018. Nat. Commun. 9, 191–203.
Filipe, V., Hawe, A., Jiskoot, W., 2010. Pharmaceut. Res. 27, 796–810.
He, L., Smith, E.A., Natan, M.J., Keating, C.D., 2004. J. Phys. Chem. B 108 (30), 10973–10980.
Hosseini-Beheshti, E., Pham, S., Adomat, H., Li, N., Tomlinson, E.S., 2012. Mol. Cell. Proteomics 11, 863–885.
Ibsen, S.D., Wright, J., Lewis, J.M., Kim, S., Ko, S.Y., Ong, J., Manouchehri, S., Vyas, A., Akers, J., Chen, C.C., Carter, B.S., Esener, S.C., Carter, B.S., 2017. ACS Nano 11, 6641–6651.
Jakobsen, K.R., Paulsen, B.S., Bæk, R., Varming, K., Sorensen, B.S., Jørgensen, M.M., 2015. J. Extracell. Vesicles 4, 26659–26668.
Jiang, Y., Shi, M., Liu, Y., Wan, S., Cui, C., Zhang, L., Tan, W.H., 2017. Angew. Chem. Int.

Ed. 56 (39), 11916–11920.
Lee, J.H., Kim, J.A., Kwon, M.H., Kang, J.Y., Rhee, W.J., 2015. Biomaterials 54, 116–125.
Li, A., Zhang, T., Zheng, M., Liu, Y., Chen, Z., 2017a. J. Hematol. Oncol. 10, 175–183.
Li, Q., Tofaris, G.K., Davis, J.J., 2017b. Anal. Chem. 89, 3184–3190.
Liu, N., Liedl, T., 2018. Chem. Rev. 118, 3032–3053.
Liu, R.J., Wang, Q., Li, Q., Yang, X.H., Wang, K.M., Nie, W.Y., 2017. Biosens. Bioelectron. 87, 433–438.
Mathivanan, S., Ji, H., Simpson, R.J., 2010. Journal of Proteomics 73, 1907–1920.
Nie, W., Wang, Q., Yang, X., Zhang, H., Li, Z., Gao, L., Zheng, Y., Liu, X., Wang, K., 2017. Anal. Chim. Acta 993, 55–62.
Park, J., Hwang, M., Choi, B., Jeong, H., Jung, J.H., Kim, H.K., Hong, S., Park, J., Choi, Y., 2017. Anal. Chem. 89, 6695–6701.
Raposo, G., Stoorvogel, W., 2013. JCB (J. Cell Biol.) 200, 373–383.
Steinbichler, T.B., Dudás, J., Riechelmann, H., Skvortsova, I.I., 2017. Semin. Canc. Biol. 44, 170–181.
Subra, C., Laulagnier, K., Perret, B., Record, M., 2007. Biochimie 89, 205–212.
Thakur, A., Qiu, G., Siu-Pang, N.G., Guan, J., Yue, J., Lee, Y., Wu, C.M.L., 2017. Biosens. Bioelectron. 94, 400–407.
Théry, C., Amigorena, S., Raposo, G., Clayton, A., 2006. Current Protocols in Cell Biology. (Chapter 3): Unit 3 22.
Théry, C., Ostrowski, M., Segura, E., 2009. Nat. Rev. Immunol. 9, 581–593.
Théry, C., Zitvogel, L., Amigorena, S., 2002. Nat. Rev. Immunol. 2, 569–579.
Tuerk, C., Gold, L., 1990. Science 249, 505–510.
Wang, Q., Li, Q., Yang, X.H., Wang, K.M., Du, S.S., Zhang, H., Nie, W.Y., 2016a. Biosens. Bioelectron. 77, 1001–1007.
Wang, Q., Liu, R.J., Yang, X.H., Wang, K.M., Li, Q., Zhu, J.Q., 2016b. Sensor. Actuator. B Chem. 223, 613–620.
Wang, Q., Luo, B., Yang, X., Wang, K.M., Liu, L., Du, S.S., 2016c. J. Mol. Recognit. 29, 151–158.
Wang, J., Lu, Z., Tang, H., Wu, L., Wang, Z., Wu, M., Yi, X., Wang, J., 2017a. Anal. Chem. 89, 10834–10840.
Wang, S., Zhang, L., Wan, S., Cansiz, S., Cui, C., Liu, Y., Wu, Y., Dong, Y., Tan, W.H., 2017b. ACS Nano 11, 3943–3949.
Wang, Y.M., Liu, J.W., Adkins, G.B., Shen, W., Trinh, M.P., Duan, L.Y., Jiang, J.H., Zhong, W., 2017c. Anal. Chem. 89, 12327–12333.
Wang, Z., Zong, S., Wang, Y., Li, N., Li, L., Lu, J., Wang, Z., Chen, B., Cui, Y., 2018. Nanoscale 10, 9053–9062.
Wu, B., Jiang, R., Wang, Q., Huang, J., Yang, X., Wang, K., Li, W., Chen, N., Li, Q., 2016. Chem. Commun. 52, 3568–3571.
Wubbolts, R., Leckie, R.S., Veenhuizen, P.T., Schwarzmann, G., Möbius, W., Hoernschemeyer, J., Stoorvogel, W., 2003. J. Biol. Chem. 278, 10963–10972.
Wunsch, B.H., Smith, J.T., Gifford, S.M., Wang, C., Brink, M., Bruce, R.L., Austin, R.H., Stolovitzky, G., Astier, Y., 2016. Nat. Nanotechnol. 11, 936–942.
Xia, Y., Liu, M., Wang, L., Yan, A., He, W., Chen, M., Lana, J., Xu, J., Guan, L., Chen, J., 2017. Biosens. Bioelectron. 92, 8–15.
Yang, Z., Ding, X., Guo, Q., Wang, Y., Lu, Z., Ou, H., Luo, Z., Lou, X., 2017. Sensor. Actuator. B Chem. 253, 1129–1136.
Yi, X., Hao, Y., Xia, N., Wang, J., Quintero, M., Li, D., Zhou, F., 2013. Anal. Chem. 85, 3660–3666.
Zhang, W., Xia, W., Lv, Z., Xin, Y., Ni, C., Yang, L., 2017. Cell. Physiol. Biochem. 41, 755–768.
Zhou, Q., Rahimian, A., Son, K., Shin, D.S., Patel, T., Revzin, A., 2016a. Methods 97, 88–93.
Zhou, Y.G., Mohamadi, R.M., Poudineh, M., Kermanshah, L., Ahmed, S., Safaei, T.S., Stojcic, J., Nam, R.K., Sargent, E.H., Kelley, S.O., 2016b. Small 12, 727–732.
Zhu, L., Wang, K., Cui, J., Liu, H., Bu, X., Ma, H., Wang, W.Z., Gong, H., Lausted, C., Hood, L., Yang, G., 2014. Anal. Chem. 86, 8857–8864.
Zou, G., Benktander, J.D., Gizaw, S.T., Gaunitz, S., Novotny, M.V., 2017. Anal. Chem. 89, 5364–5372.